PCCP

PAPER

View Article Online
View Journal

Cite this: DOI: 10.1039/c4cp05089d

Enhancement and extinction effects in surface-enhanced stimulated Raman spectroscopy

B. X. K. Chng,[ab] T. van Dijk,[a] R. Bhargava[ac] and P. S. Carney*[ab]

Received 4th November 2014,
Accepted 2nd March 2015

DOI: 10.1039/c4cp05089d

www.rsc.org/pccp

We address the optical physics of surface-enhanced stimulated Raman spectroscopy (SESRS) from the microscopic to macroscopic scales to provide experimental design criteria in colloidal-suspension SESRS. The nanoparticles that provide local field enhancement also extinguish the Raman signal. We compute the total Raman signal detected from a suspension of Raman-active molecules and nanoparticles due to the cumulative effects of enhancement and extinction and find optimum operating parameters for pump frequency and nanoparticle concentration.

1 Introduction

Raman scattering provides access to the vibrational states of molecules through spectroscopic optical experiments.[1] However, the Raman signal that is detected is generally weak and so several methods have been developed to boost the detected Raman signal. In surface-enhanced Raman spectroscopy (SERS), the Raman signal, the intensity of the Stokes field, is enhanced by placing the Raman-active molecule near some metal or plasmonic nanoparticles. Alternatively, the efficiency of the light–molecule interaction can be improved by adding an applied field at the Stokes frequency to produce stimulated Raman scattering (SRS) instead. Combining these methods, the local field enhancement of the stimulated process is expected to be larger than the local field enhancement of the spontaneous process because both the pump and seed field are amplified in the stimulated process. An experimental realization of these ideas with ultrafast pulses has recently been demonstrated.[2]

Surface enhancement of Raman scattering has been widely deployed in applications such as ultra-sensitive detection and multiplexed analyses in biological samples.[3–9] However, much of the research and application in this area are focused on the exploitation of spontaneous Raman scattering on the surface of a nanoparticle that provides the local field enhancement.[10–13]

As in spontaneous Raman scattering, the enhancement increases with the number of nanoparticles and as the plasmon resonance is approached. However, the presence of the nanoparticle also attenuates the signal through absorption and scattering. Despite the local field enhancements, these absorption and scattering phenomena ultimately lead to the extinction of the Raman signal. It has been shown[14] that competition between the enhancement and extinction effect on the Raman signal in surface-enhanced Raman spectroscopy (SERS) ultimately limits the signal gain and leads to optimal concentration and incident frequency.

Here we address the effects of enhancement and extinction for surface-enhanced stimulated Raman spectroscopy (SESRS). The enhancement and extinction effects on SESRS due to metallic nanoparticles are examined and then applied to a suspension of nanoparticles by effective medium theory. It is demonstrated that the effect of local field enhancement in SESRS is expected to be larger than in conventional SERS. Competition between enhancement and extinction ultimately leads to peak Raman signals off the plasmon resonance of the nanoparticles. Moreover, optimum nanoparticle concentrations emerge from the theory.

2 Enhancement

In this section, we compute the enhancement factor for two important specific examples: spheres and dimers. More general cases may be treated by extension of these methods.

2.1 Enhancement due to single sphere

To understand SESRS with a collection of nanoparticles, we consider the enhancement and extinction of the Raman-scattered field due to a single sphere with radius much smaller than the wavelength of interest. A Raman-active molecule is assumed to be located on the surface of the sphere and is

[a] Beckman Institute for Advanced Science and Technology, University of Illinois at Urbana-Champaign, 405/N Mathews Ave, Urbana, IL 61801, USA. E-mail: carney@illinois.edu
[b] Department of Electrical and Computer Engineering, University of Illinois at Urbana-Champaign, Urbana, IL 61801, USA
[c] Department of Bioengineering, University of Illinois at Urbana-Champaign, Urbana, IL 61801, USA

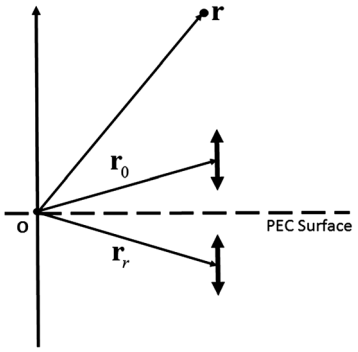

Fig. 1 Illustrating the position of the dipole, its image and the point of observation in eqn (2). The total Stokes field $\mathbf{E}_R(\omega)$ at position $\mathbf{r}$ is the sum of the field from the dipole (depicted by the double-arrow line) at position $\mathbf{r}_0$ and the scattered field from the image dipole at position $\mathbf{r}_r$.

modeled as a single induced dipole near the surface of a perfect electric conductor (PEC). The polarizability of the molecule is

$$\alpha = 6\varepsilon_0\chi_m^{(3)}|\mathbf{E}_p|^2, \quad (1)$$

where $\chi_m^{(3)}$ is the hyper-polarizability,[15] $\mathbf{E}_p$ is the electric field amplitude of the pump beam and ε_0 is the permittivity of free space.

We follow closely the calculation of the enhancement factor by Kerker.[16] Consider the radiation from the dipole located at position $\mathbf{r}_0$ in the presence of the sphere and induced through a four-wave mixing process by the incident pump beam $\mathbf{E}_p$ and Stokes beam $\mathbf{E}_s$. We assume that $|\mathbf{E}_p|^2$ does not vary significantly of the size scale of the sphere. The dipole is excited by both the pump field $\mathbf{E}_p$ and the Stokes field $\mathbf{E}_s$, the total Stokes field $\mathbf{E}_R(\omega)$ at position $\mathbf{r}$ is

$$\mathbf{E}_R(\mathbf{r},\omega) = \alpha\mathbf{G}_0(\mathbf{r},\mathbf{r}_0,\omega)\cdot\mathbf{E}_s(\mathbf{r}_0) + \alpha g a^3 \times \mathbf{G}_0(\mathbf{r},\mathbf{r}_r,\omega)\cdot[\mathbf{G}_0(\mathbf{r}_r,\mathbf{r}_0,\omega)\cdot\mathbf{E}_s(\mathbf{r}_0)], \quad (2)$$

where $\mathbf{G}_0(\mathbf{r},\mathbf{r}_0,\omega)$ is the free-space, dyadic Green function[17] for the Stokes field, $\mathbf{r}_r$ is the position of the image dipole, $g = (p^2 - 1)/(p^2 + 2)$ and $p = m_s/m$ is the ratio of the refractive index of the sphere to the refractive index of the medium at the Stokes frequency. The geometry for eqn (2) is depicted in Fig. 1. The first term on the right-hand side of eqn (2) represents the contribution to $\mathbf{E}_R(\omega)$ from the dipole at $\mathbf{r}_0$ and the second term represents the contribution to $\mathbf{E}_R(\omega)$ from the image dipole at $\mathbf{r}_r$.

Eqn (2) depends on the orientation of the dipole and so the scattered Stokes field $\mathbf{E}_R(\mathbf{r},\omega)$ depends on the azimuthal and polar angle of the dipole orientation. The enhanced fields at the surface of metallic nanoparticles are nearly normal to the surface.[18] The induced dipole of the molecule will thus tend to be normal to the surface as well. In the special case when the dipole is oriented normal to the surface, that is, radially,[16] eqn (2) simplifies to

$$\mathbf{E}_R(\mathbf{r},\omega) = \alpha|1 + 2g_0|^2(1 + 2g)^2\mathbf{E}_s^{(0)}(\mathbf{r}), \quad (3)$$

where $\mathbf{E}_s^{(0)}(\mathbf{r})$ is the scattered field in the absence of the sphere and g_0 is g evaluated at the pump field frequency. Thus the scattered field in the far zone of a dipole located at the surface of the sphere is equivalent to the scattered field of the dipole in the absence of the sphere multiplied by the enhancement factor $|1 + 2g_0|^2(1 + 2g)^2$. We define the enhancement factors on the pump and Stokes fields as $f_p = (1 + 2g_0)$ and $f_s = (1 + 2g)$ respectively.

If the hyperpolarizability of the molecule is extremely anisotropic, the dipole induced may have components parallel to the surface of the nanoparticle. For molecules close to the surface, the fields radiated from those components of the dipole are damped rather than enhanced, leading to some overall reduction in the enhancement. This factor by which the enhancement is reduced is of order one unless the molecules are preferentially bound to the particle so that the induced dipole is predominantly oriented parallel to the surface. In this case the analysis presented here is moot. We thus assume that the dipoles are all normal to the surface and that averaging over positions on the sphere does not significantly change the enhancement factor.[19] The enhancement of the intensity of the Stokes field in SESRS for a monolayer of Raman-active molecules on the surface of a metallic nanoparticle is thus

$$G = ||f_p|^2 f_s^2|^2. \quad (4)$$

Compared to the expression for the enhancement factor derived in the work of van Dijk *et al.*,[14] we see that the enhancement factor for SESRS is the square of the enhancement factor in SERS. Thus, for a single sphere, not only does SRS improve the efficiency of the Raman scattering process, but the effects of surface enhancement in SESRS provide an even larger improvement compared to SRS than that which SERS provides compared to spontaneous Raman scattering.

2.2 Enhancement due to dimer

Let us consider dimers that consist of two spheres with equal radius a that are separated by a gap d. To calculate the average enhancement factor G_{dimer} of a nanospherical dimer, we consider the enhancement factor in two distinct regions that are depicted in Fig. 2. The first region (a) is denoted as the hot spot where

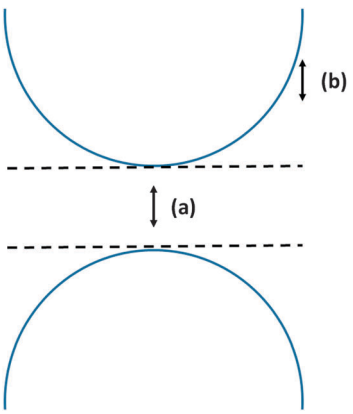

Fig. 2 Illustration of the nanospherical dimer and the two regions of interest. The region labelled by (a) is the hot spot where the Raman signal is significantly enhanced. The region labelled by (b) experiences enhancement that is similar to the single sphere case.

significant enhancement on the order of 10^8–10^{11} has been reported.[20,21] The second region (b) experiences enhancement that is similar to the single sphere case because the interaction between this region and the adjacent dimer is small compared to the interaction between region (a) and the adjacent dimer. This allows us to calculate the enhancement factor G_b in region (b) by using eqn (4). The enhancement factor in region (a) is calculated by appealing to the RLC model[20] where the hot spot is modeled as a capacitor and the spheres are modeled by an effective inductance R–L. The induced charge on the dimer surface due to some incident field E_0 is given by

$$\sigma_s = E_0 \frac{p^2 - 1}{p^2 + \beta}(1 + \beta), \tag{5}$$

where β is the size ratio given by $\beta = (2a)/d$. By assuming that the radius a of the sphere is larger than the gap d, we can approximate the gap as a parallel-plate capacitor where the plates are denoted by the dashed line in Fig. 2. As a result, the enhancement of the incident field inside the gap is

$$g_{dim} = \frac{p^2 - 1}{p^2 + \beta}\frac{1 + \beta}{m^2}. \tag{6}$$

With the enhancement factor of each field in the four-wave mixing process, we can derive the total enhancement factor G_a in the hot spot as

$$G_a = |g_{dim}(\omega)g_{dim}(\omega_0)|^4, \tag{7}$$

The average enhancement factor G_{dimer} is taken as a weighted sum of the enhancement factor G_a and G_b. According to the analysis by Fang *et al.*,[22] the effective area of the hot spot with enhancement factor between 10^9–10^{10} is about 0.006% of the total surface area of the dimer. This gives us an average enhancement factor of

$$G_{dimer} = 10^{-6}G_a + (1 - 10^{-6})G_b. \tag{8}$$

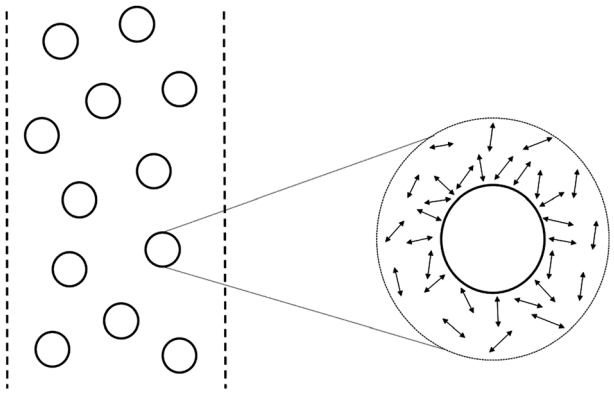

Fig. 3 Illustration of the composite medium consisting of nanoparticles embedded in a dielectric. A slab with thickness h, refractive index m and negligible third-order susceptibility is filled with particles that are well approximated by spheres. The slab is also filled with Raman-active molecules depicted by the double-arrow lines. Only the molecules near the particle will see a profound enhancement induced by the presence of the particle.

2.3 Enhancement due to slab of nanoparticles

Next we develop an effective medium for the four-wave mixing, or Raman, susceptibility $\chi^{(3)}_{eff}$ in a colloidal suspension of nanoparticles and Raman-active molecules. The composite medium in the SESRS experiment is depicted in Fig. 3. The slab, with thickness h and refractive index m, is filled with Raman-active molecules and nanoparticles. The enhancement of the scattered Stokes field is profound only for Raman-active molecules that are near the sphere. Thus, we consider only molecules at the surface of the spheres as above. We assume that the positions of the molecules are uncorrelated so that the interactions of the fields between the molecules can be neglected.[23,24] We replace the sphere surrounded by these Raman-active molecules by an equivalent dipole with a hyper-polarizability $\chi^{(3)}_{sph}$. The explicit expression for the total Stokes field $\mathbf{E}_R(\mathbf{r},\omega)$ due to a monolayer of Raman-active molecules attached to a sphere is given by

$$\mathbf{E}_R(\mathbf{r},\omega) = N\alpha|f_p|^2 f_s^2 \mathbf{E}_s^{(0)}(\mathbf{r}), \tag{9}$$

where N is the number of Raman-active molecules attached to the sphere. From eqn (9), we see that the total Stokes field from a monolayer on a sphere is equivalent to the total Stokes field from a dipole if we define the hyper-polarizability $\chi^{(3)}_{sph}$ of the latter as

$$\chi^{(3)}_{sph} = Nf_s^2|f_p|^2\chi^{(3)}_m. \tag{10}$$

Consider a slab filled with a distribution of identical dipoles with hyper-polarizability $\chi^{(3)}_{sph}$ such that the separation between these dipoles is much smaller than the wavelength of light at frequencies of interest. We then consider a sphere with radius R that is smaller than the wavelengths of interest within the slab. This sphere (which is a fictitious construct) encompasses some of the dipoles and is depicted in Fig. 4 by the dotted circle. Within the effective medium approximation,[23,25] we can replace the region in this sphere with a homogeneous medium. The susceptibility of the homogeneous medium $\chi^{(3)}_{eff}$ is related to $\chi^{(3)}_{sph}$ by the following relation:

$$\chi^{(3)}_{eff} = \rho\chi^{(3)}_{sph}, \tag{11}$$

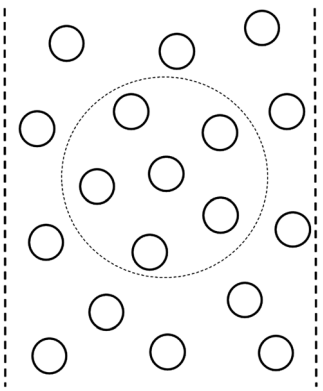

Fig. 4 Construction of a fictitious sphere inside the slab that encompasses some of the particles. The field scattered from the collection of particles within the sphere will be considered during the homogenization process.

where ρ is the number density of particles within the slab. If we then substitute eqn (10) into (11), we obtain the effective Raman susceptibility of the homogeneous medium in terms of the hyper-polarizability of the Raman-active molecules as

$$\chi^{(3)}_{\text{eff}} = \rho\langle N\rangle f_s^2 f_p f_p^* \chi^{(3)}_m. \tag{12}$$

3 Extinction

In this section, we consider the extinction processes for a slab of nanoparticles. Two specific nanoparticles are considered: spheres and dimers.

3.1 Extinction due to slab of single spheres

First, we deal with the extinction processes in such a slab. The electric field $\mathbf{E}_t$ transmitted through the slab of nanoparticles is given by the sum of the incident field $\mathbf{E}_i$ and the corresponding field scattered from each nanoparticle in the slab. Evaluating this sum in the far zone, the transmitted field is approximately related to the incident field by the equation,[26]

$$\mathbf{E}_t = \mathbf{E}_i \exp\left[-\frac{2\pi m\rho h}{k^2} S(0)\right], \tag{13}$$

where h is the thickness of the slab and $S(0)$ is the scattering amplitude of the electromagnetic fields in the forward direction. The transmission coefficient of a homogeneous slab of thickness h and refractive index $\tilde{m}$ is well-known and is given by[26]

$$\tilde{t}_{\text{slab}} = \frac{\mathbf{E}_t}{\mathbf{E}_i} = e^{i\frac{2\pi}{\lambda}(\tilde{m}-m)h}. \tag{14}$$

Comparing eqn (13) and (14), the field in the far-zone transmitted through a homogeneous slab is equivalent to the field scattered by a slab of particles for $\tilde{m}$ given by

$$\tilde{m} = m\left[1 + i\frac{2\pi\rho}{k^3} S(0)\right]. \tag{15}$$

With the effective refractive index of the slab of particles, the intensity of the transmitted field can be derived using Beer's law which is well-understood in the context of a homogeneous medium.[27] The attenuation coefficient γ that appears in Beer's law is given by

$$\gamma = 2k\,\text{Im}\,\tilde{m}. \tag{16}$$

The optical theorem[26] relates the forward scattering amplitude and the cross-section,

$$C_{\text{ext}} = \frac{4\pi}{k^2}\text{Re}[S(0)]. \tag{17}$$

Thus from eqn (15) into (16), the effective attenuation of the slab of nanoparticles is

$$\gamma = m\rho C_{\text{ext}}. \tag{18}$$

Thus the attenuation coefficient γ can be described by the extinction cross-section C_{ext} which, in turn, may be computed from the partial wave, or Mie, coefficients.[26] Since the sphere is assumed to be much smaller than the wavelength of interest, contributions from terms of higher order in the radius a are neglected. The extinction cross-section for a small metallic sphere for a field of wavenumber $k = \omega/c$, to powers of $(ka)^4$ is

$$\begin{aligned} C_{\text{ext}} &= 4k\pi a^3 \text{Im}\left\{\frac{p^2-1}{p^2+2}\left[1 + \frac{(ka)^2}{15}\frac{p^2-1}{p^2+2}\right.\right. \\ &\quad \left.\left. \times \frac{p^4+27p^2+38}{2p^2+3}\right]\right\} \\ &\quad + \frac{8}{3}(ka)^4\pi a^2 \text{Re}\left[\left(\frac{p^2-1}{p^2+2}\right)^2\right], \end{aligned} \tag{19}$$

where $p = m_s/m$ is the ratio of the refractive index of the sphere, m_s to the refractive index of the medium, m where the sphere is embedded.

3.2 Extinction due to slab of dimers

We calculate the extinction cross-section $C_{\text{ext,dimer}}$ of a nanospherical dimer with geometry as shown in Fig. 2. We make the Rayleigh–Gans approximation so that multiple scattering interactions between spheres can be ignored. Within this approximation, the total extinction cross-section of an arbitrary cluster $C_{\text{ext,tot}}$ consisting of N spheres is given by[28]

$$C_{\text{ext,tot}} = \sum_{i=1}^{N} C^{(i)}_{\text{ext}}, \tag{20}$$

where $C^{(i)}_{\text{ext}}$ is the extinction cross-section of the ith sphere. In the case of a dimer ($N = 2$), the extinction cross-section is

$$C_{\text{ext,dimer}} = 2C_{\text{ext}}, \tag{21}$$

where C_{ext} is given by eqn (19). The effective attenuation γ_{dimer} of a slab of nanospherical dimers is calculated using the same formalism in Section 3.1 so that

$$\gamma_{\text{dimer}} = m\rho C_{\text{ext,dimer}}. \tag{22}$$

4 Combined model

In this section, we combine the results derived in Sections 2 and 3 to obtain the cumulative effects of enhancement and extinction due to the presence of the nanoparticles on the total Raman signal R in the far zone, depicted schematically in Fig. 6.

We assume that the pump and the applied Stokes field are strong in the sense that the applied Stokes field is much larger than the scattered Stokes field and the pump does not change significantly absent the linear absorption introduced by the nanoparticles. The coupled wave equations[15] for stimulated Raman scattering were solved numerically using the hyper-polarizability, $\chi^{(3)}_{\text{eff}}$, derived from effective medium approach above. We take $G = 10^{12}$ and $\rho = 1$ nM as shown in Fig. 5. These values are realistic for the enhancement factors and concentration of nanoparticles used in an experiment.[14,16] It can be seen from the figure that the intensity of the pump field for the given parameters decreases slowly over the sample and falls to 90% of its initial value over 2 mm. This size scale is

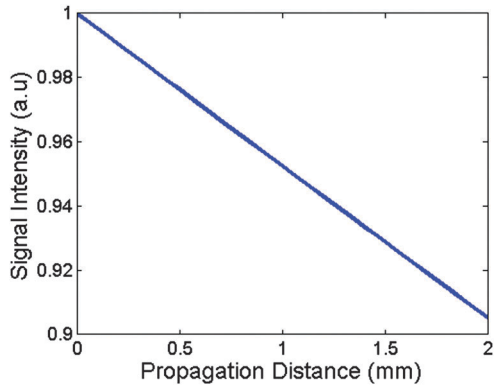

Fig. 5 Predicted intensity of pump field against the propagation distance z. The signal is plotted for $G = 10^{12}$ and concentration of $\rho = 1$ nM. The pump field is normalized with respect to its maximum value taken over the range of z from $z = 0$ mm to 2 mm.

typically encountered when the sample of interest is contained in a cuvette.

To include the effects of extinction,[14] we incorporate Beer's law to the propagation of the pump and Stokes field through a slab of spheres of thickness $z = h$ by including extinction terms in the coupled-wave equations. The modified coupled-wave equations for SRS including extinction take the form

$$\frac{\mathrm{d}A_\mathrm{s}}{\mathrm{d}z} = 3i\omega\frac{\rho\langle N\rangle\sqrt{G}\chi_\mathrm{m}^{(3)}}{mc}|A_\mathrm{p}|^2A_\mathrm{s} - \frac{1}{2}\rho mC_\mathrm{ext}(\omega)A_\mathrm{s}, \tag{23}$$

$$\frac{\mathrm{d}A_\mathrm{p}}{\mathrm{d}z} = -\frac{1}{2}\rho mC_\mathrm{ext}(\omega_0)A_\mathrm{p}, \tag{24}$$

where A_p and A_s are the amplitudes of the pump and Stokes' field respectively. The total Raman signal is obtained by solving for the Stokes' field amplitude in eqn (23) and (24) and using the intensity formula $R = \frac{1}{2}m\varepsilon_0c|\mathbf{E}_\mathrm{R}|^2$ to obtain

$$R = I_\mathrm{s}(0)\left|\exp\left[6i\omega I_\mathrm{p}(0)\frac{\langle N\rangle\sqrt{G}\chi_\mathrm{m}^{(3)}}{m^2\varepsilon_0c^2}\left(\frac{1-\mathrm{e}^{-\rho mC_\mathrm{ext}(\omega_0)h}}{mC_\mathrm{ext}(\omega_0)}\right) - \frac{1}{2}\rho mC_\mathrm{ext}(\omega)h\right]\right|^2, \tag{25}$$

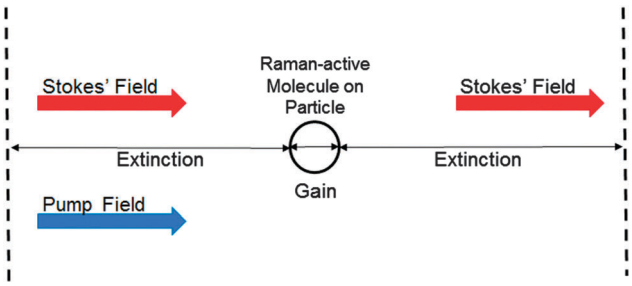

Fig. 6 Model for including the effects of enhancement and extinction together. The incident pump and Stokes field will experience extinction as they propagate through the sample until it interacts with a Raman active molecule on a particle. The scattered Stokes field will be enhanced by this interaction and experiences further extinction as it propagates out of the sample.

where $I_\mathrm{p}(0)$ and $I_\mathrm{s}(0)$ are the initial pump and Stokes' intensities respectively. From this expression, we see that the Raman signal is determined by two competing processes: the enhancement and the extinction. A similar competition is seen in SERS.[14] However, we see an exponential dependence on both the enhancement and extinction cross-section for SESRS as compared to a linear dependence on the enhancement for SERS. The process that increase the enhancement effects also increases the overall extinction effects on the Raman signal.

If the interaction length is small such that the exponent in eqn (25) is much less than unity, a simpler expression can be obtained through linearization. Taking the Taylor expansion of eqn (25) and keeping terms quadratic in the exponent such that we are only considering SESRS, we obtain the following expression,

$$R = \langle N\rangle^2R^{(0)}G\mathrm{e}^{-\rho mC_\mathrm{ext}(\omega)h}\left(\frac{1-\mathrm{e}^{-\rho mC_\mathrm{ext}(\omega_0)h}}{mC_\mathrm{ext}(\omega_0)}\right)^2, \tag{26}$$

where $R^{(0)}$ is the Raman signal due to a single Raman-active molecule without the presence of the sphere.

Alternatively, eqn (26) can be derived by considering the SRS interaction within the first Born approximation.[14] The pump and Stokes beam incident on the slab will be attenuated upon propagation until they interact with the Raman-active molecules. The interaction with the molecules will produce the Stokes field that is enhanced by the factor G due to the presence of the sphere. The scattered field is then further attenuated as it propagates through the medium to $z = h$. By incorporating these effects and using the intensity formula, the total Raman signal becomes

$$\begin{aligned} R = {} & \langle N\rangle^2AR^{(0)}G\left(\int_0^h\mathrm{d}z\rho(z)\exp\left[-\int_0^z\mathrm{d}z'\rho(z')mC_\mathrm{ext}(\omega)/2\right]\right. \\ & \times\exp\left[-\int_0^z\mathrm{d}z'\rho(z')mC_\mathrm{ext}(\omega_0)\right] \\ & \left.\times\exp\left[-\int_z^h\mathrm{d}z'\rho(z')mC_\mathrm{ext}(\omega)/2\right]\right)^2, \end{aligned} \tag{27}$$

If the number density of particles ρ does not depend on its spatial coordinates, the integrals in eqn (27) can be evaluated in close form to give eqn (26).

5 Simulations and discussion

Using eqn (25), we plot the Raman signal for a slab of single sphere nanoparticles as a function of wavelength and concentration to analyze the competing effects of enhancement and extinction in SESRS. These plots were generated using the optical constants of gold with a plasmon resonance of about 520 nm that were obtained by Johnson and Christy[29] and are shown in Fig. 7. Likewise, results for silver and copper nanoparticles can be obtained from the data in Johnson and Christy.[29] In Fig. 7a, it is clearly seen that the peak signal gets shifted further away from the plasmon resonance as the concentration of the particles is increased. Hence, the significant

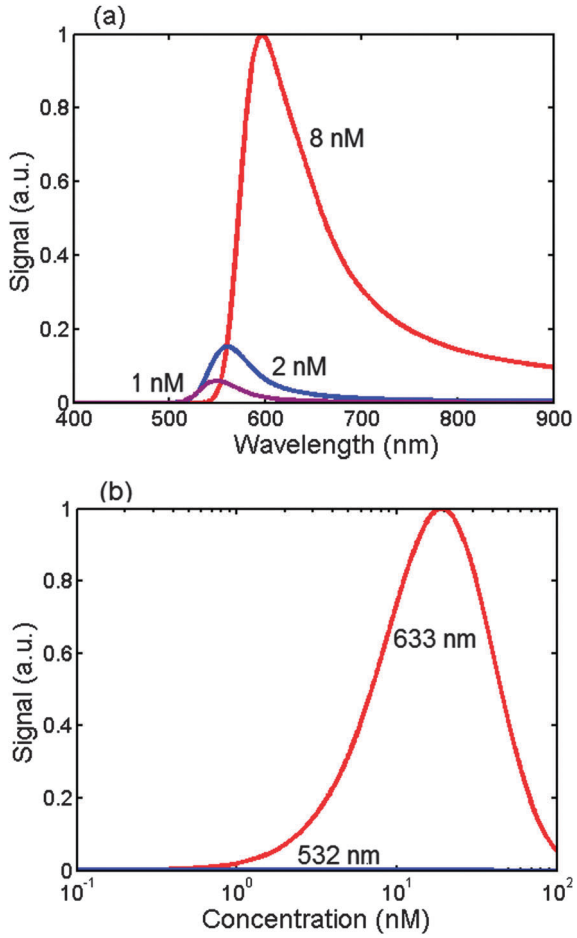

Fig. 7 Predicted signal for SESRS in transmission mode as a function of (a) the wavelength of incident light. The signals are plotted at three different concentrations of gold nanospheres with a radius of 15 nm. The thickness of the suspension h is 1 mm. Predicted signal for SESRS as a function of (b) the concentration of gold nanospheres. The signals are plotted at two incident wavelength (532 nm and 633 nm). The radius of the gold nanospheres is 20 nm and the thickness of the suspension h is 1 mm.

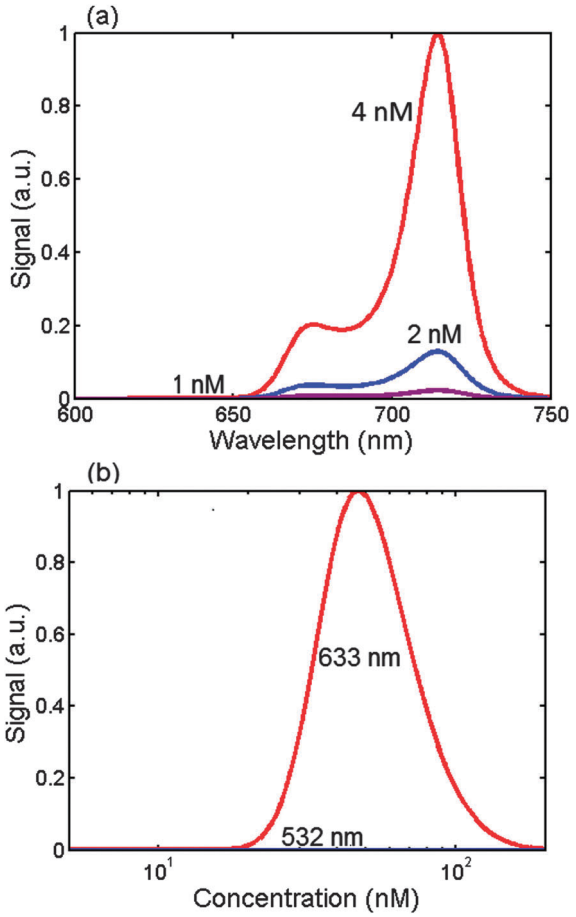

Fig. 8 Predicted signal for SESRS using nanoparticle dimers in transmission mode as a function of (a) the wavelength of incident light. The signals are plotted at three different concentrations of gold nanospheres with a radius of 20 nm and a gap of 5 nm between the nanospheres. The thickness of the suspension h is 100 μm. Predicted signal for SESRS as a function of (b) the concentration of gold nanospheres. The signals are plotted at two incident wavelength (532 nm and 633 nm). The radius of the gold nanospheres is 20 nm with a gap of 5 nm between the nanospheres and the thickness of the suspension h is 1 mm.

enhancement effect at the plasmon resonance is negated by the strong extinction effects near the plasmon resonance such that no appreciable signal is obtained.

Fig. 7b depicts the relationship between the Raman signal and the concentration for two commonly used incident wavelengths evaluated at the Raman band of 1076 cm^{-1}. For λ = 532 nm, the signal is almost negligible because the incident wavelength is very close to the plasmon resonance of the nanoparticle. On the other hand, the signal for λ = 633 nm is much stronger and it can be clearly seen from this incident wavelength that there is a non-linear relationship between the intensity of the Raman signal and the concentration of enhancement particles. Due to the competition between the enhancement and extinction effects, there is an optimal concentration ρ_{opt} where the extinction effects are balanced by the strong enhancement effects from the nanoparticles.[14] This optimal concentration can be found by taking the derivative of eqn (26) and setting the resultant expression to zero. We find that ρ_{opt} takes the form

$$\rho_{opt} = \frac{\ln\left[\dfrac{12\omega I_p(0)\langle N\rangle\sqrt{G}\,\mathrm{Re}\left[\chi_m^{(3)}\right]}{m^3\varepsilon_0 c^2 C_{ext}(\omega)}\right]}{mhC_{ext}(\omega_0)}. \quad (28)$$

Hence, the non-linear relationship between the Raman signal and the concentration of nanoparticles is a crucial factor in the experimental design. In particular, eqn (28) provides a method for optimizing the total Raman signal collected through varying the nanoparticle concentration. This relation also provides caution to the notion that one can increase the concentration of nanoparticles in the hopes of strengthening the Raman signal since the extinction effects will dominate beyond a certain critical point.

Due to the non-linear interaction in SESRS, we find that the optimum concentration is dependent on the enhancement

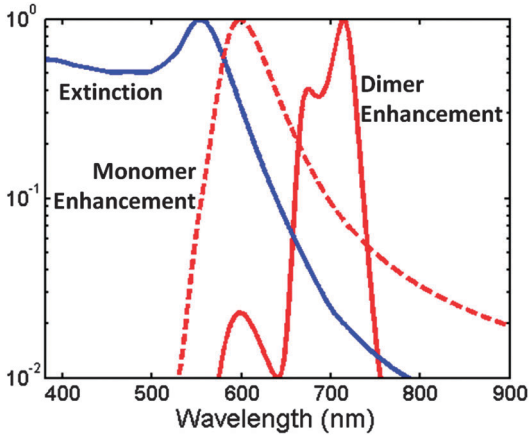

Fig. 9 (solid blue) The normalized extinction cross-sections C_{ext} and $C_{ext,dimer}$ plotted using single gold spheres with a radius of 20 nm and gold dimers with a radius of 20 nm and a gap of 5 nm as a function of the incident wavelength respectively. The normalized extinction cross-section for monomers lies on top of the extinction cross-section for dimers since the two quantities differ by some scalar factor only. (dashed red) The normalized enhancement factor G plotted using single gold spheres with a radius of 20 nm as a function of the incident wavelength. (solid red) The normalized average enhancement factor G_{dimer} plotted using gold dimers with a radius of 20 nm and a gap of 5 nm as a function of the incident wavelength. The plots of the enhancement factors are evaluated for a Raman shift of 1076 cm^{-1}.

factor and the extinction cross-sections in contrast to SERS where the optimum concentration is dependent on the extinction cross-sections only.[14] In comparison, the optimum concentration for the linearized equation, eqn (26), is

$$\rho_{opt} = \frac{\ln\left[1 + \frac{2C_{ext}(\omega_0)}{C_{ext}(\omega)}\right]}{mhC_{ext}(\omega_0)}. \quad (29)$$

Like SERS, the optimum concentration in the linearized regime is independent of the enhancement factor. We expect eqn (28) and (29) to converge as the interaction length decreases because eqn (25) will approach the linearized regime.

Likewise, we plot the Raman signal as a function of wavelength and concentration to analyze the competing effects of enhancement and extinction in SESRS with nanospherical dimers. This is obtained by using eqn (25) in conjunction with eqn (22) and (8). In Fig. 8a, it is seen that the peak signal gets shifted away from the plasmon resonance just as in the single sphere case. However, the effect of increasing nanoparticle concentration on the shifts is negligible since the resonance of the enhancement spectrum is shifted further from the resonance of the extinction spectrum as depicted in Fig. 9. This is in contrast to the single sphere case where the resonances in the enhancement and extinction spectra are close to one another so that the competition between the two effects are profound.[14]

Fig. 8b depicts the relationship between the Raman signal and the concentration of nanoparticle dimers evaluated at the Raman band of 1076 cm^{-1}. We see that the plots in Fig. 8b are similar to the plots in Fig. 7b where the signal for λ = 532 nm is

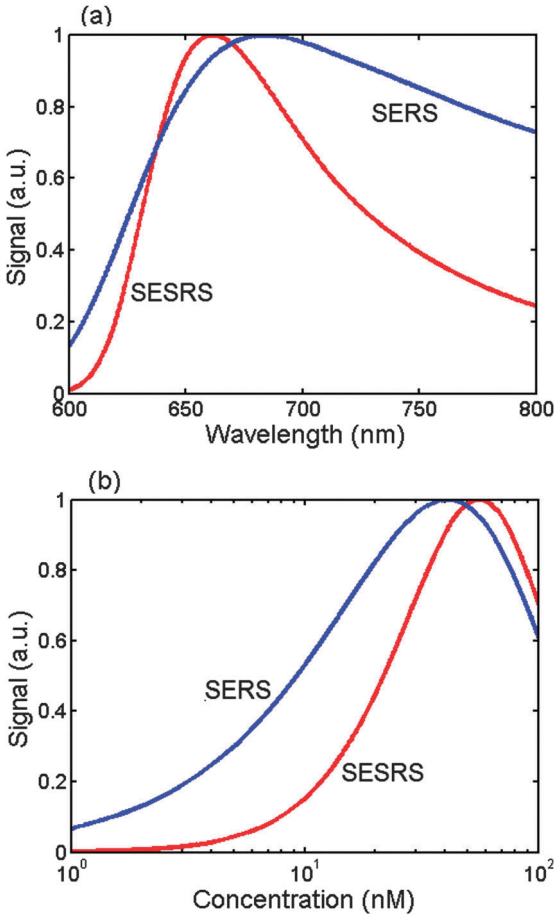

Fig. 10 Predicted signal for SESRS and SERS in transmission mode as a function of (a) the wavelength of incident light. The signals are plotted for a concentration of 8 nM and the radius of the gold nanosphere is 15 nm. Predicted signal for SESRS and SERS as a function of (b) the concentration of gold nanospheres. The signals are plotted for an incident wavelength of 633 nm and the radius of the gold nanosphere is 20 nm. Both the SESRS and SERS signals are normalized with respect to their own maximum value.

almost negligible because the incident wavelength is very close to the plasmon resonance of the nanoparticle and the signal for λ = 633 nm is much stronger. Due to the non-linear relationship between the intensity of the Raman signal and the concentration of enhancement particles, there exists an optimum concentration of nanoparticle dimers that can be calculated with the use of eqn (28).

The formalism for calculating the total Raman signal can be extended from single spheres and dimers to aggregates consisting of arbitrary spheres. This allows us to calculate the Raman signal from a suspension that consists of aggregates of varying cluster size. By characterizing the distribution of cluster size in the suspension, the total Raman signal is calculated as a weighted sum of the Raman signal from each cluster size.

Similar competition between enhancement and extinction is also seen in SERS.[14] The difference between SERS and SESRS with single sphere nanoparticles is depicted in Fig. 10. As can be seen from Fig. 10a, the peak signal in SERS is further shifted away from the plasmon resonance than the peak signal in

SESRS. That is, the competition between enhancement and extinction is more profound in SERS than in SESRS. This is expected since the huge enhancement in SESRS, which is generally larger than the enhancement effect $G_{SERS} = |f_p f_s|^2$ in SERS[14] by a factor of $|f_p f_s|^2$, helps to compensate the extinction effect.

The signals for SERS and SESRS are plotted with respect to concentration in Fig. 10b. We see that the peak signal in SERS is obtained at an appreciably lower concentration than the peak signal in SESRS. This is also indicative of the strong competition between enhancement and extinction in SERS since a lower concentration of nanoparticles is required for the extinction effects to dominate over the enhancement effects.

6 Conclusions

In this paper, we derived the results for SESRS for a suspension that is filled with Raman-active molecules and nanoparticles. The case for a suspension of singles sphere nanoparticles and for a suspension of dimer nanoparticles were considered separately. We found that the Raman enhancement factor for SESRS is in general larger than the Raman enhancement factor for SERS. This effect is desirable for the detection of the Raman signal collected from the sample. However, we see that there is competition between extinction and enhancement in the resultant Raman signal. In particular, we find that the competition between enhancement and extinction is more profound in the case with single spheres as compared to the case with dimers because the resonances in the enhancement and extinction spectra are further apart in the latter. Due to the competing effects of enhancement and extinction, the collected Raman signal does not increase arbitrarily with increasing nanoparticle concentration. Instead, there is an optimum concentration of nanoparticles, found using eqn (28). We find that a higher concentration of nanoparticles should be used in SESRS than in SERS. Likewise, in both SERS and SESRS, the optimal pump frequency is shifted away from the plasmon resonance of the nanoparticles, but that optimum is shifted even further in SERS than in SESRS.

References

1 G. C. Schatz and R. P. Van Duyne, *Handbook of Vibrational Spectroscopy*, John Wiley & Sons, Chichester, 2002, vol. 1, pp. 759–774.
2 R. R. Frontiera, A.-I. Henry, N. L. Gruenke and R. P. Van Duyne, *J. Phys. Chem. Lett.*, 2011, **2**, 1199–1203.
3 J.-X. Cheng and X. S. Xie, *Coherent Raman scattering microscopy*, CRC Press, Boca Raton, FL, 2013.
4 O. Lyandres, J. M. Yuen, N. C. Shah, R. P. VanDuyne, J. T. Walsh and M. R. Glucksberg, *Diabetes Technol. Ther.*, 2008, **10**, 257–265.
5 X. Qian, X.-H. Peng, D. O. Ansari, Q. Yin-Goen, G. Z. Chen, D. M. Shin, L. Yang, A. N. Young, M. D. Wang and S. Nie, *Nat. Biotechnol.*, 2008, **26**, 83–90.
6 G. von Maltzahn, A. Centrone, J.-H. Park, R. Ramanathan, M. J. Sailor, T. A. Hatton and S. N. Bhatia, *Adv. Mater.*, 2009, **21**, 3175–3180.
7 N. Stone, K. Faulds, D. Graham and P. Matousek, *Anal. Chem.*, 2010, **82**, 3969–3973.
8 Y. C. Cao, R. C. Jin, J. M. Nam, C. S. Thaxton and C. A. Mirkin, *J. Am. Chem. Soc.*, 2003, **125**, 14676–14677.
9 C. L. Zavaleta, B. R. Smith, I. Walton, W. Doering, G. Davis, B. Shojaei, M. J. Natan and S. S. Gambhir, *Proc. Natl. Acad. Sci. U. S. A.*, 2009, **106**, 13511–13516.
10 C. E. Talley, J. B. Jackson, C. Oubre, N. K. Grady, C. W. Hollars, S. M. Lane, T. R. Huser, P. Nordlander and N. J. Halas, *Nano Lett.*, 2005, **5**, 1569–1574.
11 A. K. Kodali, X. Llora and R. Bhargava, *Proc. Natl. Acad. Sci. U. S. A.*, 2010, **107**, 13620–13625.
12 J. B. Jackson, S. L. Westcott, L. R. Hirsch, J. L. West and N. J. Halas, *Appl. Phys. Lett.*, 2003, **82**, 257–259.
13 R. A. Alvarez-Puebla, *J. Phys. Chem. Lett.*, 2012, **3**, 857–866.
14 T. van Dijk, S. T. Sivapalan, B. M. DeVetter, T. K. Yang, M. V. Schulmerich, C. J. Murphy, R. Bhargava and P. S. Carney, *J. Phys. Chem. Lett.*, 2013, **4**, 1193–1196.
15 R. W. Boyd, *Nonlinear optics*, Academic Press, San Diego, CA, 2008.
16 M. Kerker, D. S. Wang and H. Chew, *Appl. Opt.*, 1980, **19**, 4159–4174.
17 C. Tai, *Dyadic Green Functions in Electromagnetic Theory*, IEEE Press Series on Electromagnetic Waves, IEEE Press, 1994.
18 W. L. Barnes, A. Dereux and T. W. Ebbesen, *Nature*, 2003, **424**, 824–830.
19 F. W. King and G. C. Schatz, *Chem. Phys.*, 1979, **38**, 245–256.
20 D. A. Genov, A. K. Sarychev, V. M. Shalaev and A. Wei, *Nano Lett.*, 2004, **4**, 153–158.
21 H. Xu, J. Aizpurua, M. Käll and P. Apell, *Phys. Rev. E: Stat. Phys., Plasmas, Fluids, Relat. Interdiscip. Top.*, 2000, **62**, 4318–4324.
22 Y. Fang, N.-H. Seong and D. D. Dlott, *Science*, 2008, **321**, 388–392.
23 P. Mallet, C. A. Guérin and A. Sentenac, *Phys. Rev. B: Condens. Matter Mater. Phys.*, 2005, **72**, 014205.
24 C. F. Bohren, *J. Atmos. Sci.*, 1986, **43**, 468–475.
25 J. E. Sipe and R. W. Boyd, *Phys. Rev. A: At., Mol., Opt. Phys.*, 1992, **46**, 1614–1629.
26 C. F. Bohren and D. R. Huffman, *Absorption and scattering of light by small particles*, John Wiley and Sons, New York, 1983.
27 H. C. van de Hulst, *Light scattering by small particles*, Dover Publications, 1982.
28 D. W. Mackowski, *J. Opt. Soc. Am. A*, 1994, **11**, 2851–2861.
29 P. B. Johnson and R. W. Christy, *Phys. Rev. B: Solid State*, 1972, **6**, 4370–4379.

